A Journal of

EurJIC

European Journal of Inorganic Chemistry

ChemPubSoc Europe

Accepted Article

Title: Proteins as macromolecular ligands for metal-catalysed asymmetric transfer hydrogenation of ketones in aqueous medium

Authors: José de Jesús Cázares-Marinero, Cédric Przybylski, and Michèle Salmain

This manuscript has been accepted after peer review and appears as an Accepted Article online prior to editing, proofing, and formal publication of the final Version of Record (VoR). This work is currently citable by using the Digital Object Identifier (DOI) given below. The VoR will be published online in Early View as soon as possible and may be different to this Accepted Article as a result of editing. Readers should obtain the VoR from the journal website shown below when it is published to ensure accuracy of information. The authors are responsible for the content of this Accepted Article.

To be cited as: *Eur. J. Inorg. Chem.* 10.1002/ejic.201701359

Link to VoR: http://dx.doi.org/10.1002/ejic.201701359

WILEY-VCH

10.1002/ejic.201701359

Artificial transfer hydrogenases

Dative assembling of half-sandwich ruthenium, rhodium or iridium complexes to beta-lactoglobulin and lysozyme gave biohybrids that catalyzed the asymmetric transfer hydrogenation of ketones with up to 86% *ee*. Complementary investigations pointed out to the involvement of beta-lactoglobulin's His146 in ruthenium coordination.

Accepted Manuscript

This article is protected by copyright. All rights reserved.

Proteins as macromolecular ligands for metal-catalysed asymmetric transfer hydrogenation of ketones in aqueous medium

José de Jesús Cázares-Marinero, Cédric Przybylski, Michèle Salmain*

Sorbonne Université, CNRS, Institut Parisien de Chimie Moléculaire, IPCM, F-75005 Paris, France

* to whom correspondence should be addressed. Email: michele.salmain@upmc.fr. Homepage: http://www.ipcm.fr/presentation-682?lang=en

Abstract

We report the generation of biohybrid catalysts resulting from the dative anchoring of half-sandwich organometallic complexes $[M(arene)(H_2O)_x(Cl)_y]^{n+}$ (M = Ru^{II}, arene = η^6-benzene, *p*-cymene or mesitylene; M = Ir^{III}, Rh^{III}, arene = η^5-Cp*; x = 1-3, y = 0-2, n = 0-2) to bovine beta-lactoglobulin (βLG) or hen egg white lysozyme (HEWL) with unprecedented behaviour. These constructs were shown to catalyse the asymmetric transfer hydrogenation (ATH) of aryl ketones in water with sodium formate as hydrogen donor at a much faster rate compared to the complexes alone. Full conversion of the benchmark substrate 2,2,2-trifluoroacetophenone (TFACP) was reached with enantiomeric excess (*ee*) of 86% for the most selective biohybrid. Surprisingly, even the crude biohybrid gave a good *ee* despite the presence of non-protein bound metallic species in the reaction medium. Other aryl ketones were reduced the same way, with the highest *ee* obtained for *ortho*-substituted acetophenone derivatives. Furthermore, treatment of βLG with dimethylpyrocarbonate (DMPC) resulted in a noticeable decrease of the activity and selectivity of the biohybrid, indicating that the sole accessible histidine (His146) was probably involved in the coordination and activation of Ru(benzene). This piece of work underscores that protein scaffolds are efficient chiral ligands for asymmetric catalysis. The use of sodium formate instead of dihydrogen makes this approach safe, inexpensive and environmentally friendly.

Keywords

Beta-lactoglobulin; lysozyme; artificial metalloenzyme; mass spectrometry; ruthenium

Accepted Manuscript

This article is protected by copyright. All rights reserved.

INTRODUCTION

The design of artificial metalloenzymes (ArMs) for enantioselective catalysis has been the subject of extensive research during the past fifteen years[1] and has now reached a state of maturity.[2] ArMs elegantly complement wild-type enzymes by achieving high turnover numbers and high enantioselectivity under mild conditions while expanding their application to a wider range of reactions and substrates. Various strategies are employed to implant a catalytically active metal centre within biomacromolecules such as DNA, native proteins or *de novo* peptide scaffolds. These strategies are rationalized into three distinct approaches, i.e. covalent, supramolecular and dative anchoring as well as a combination of them.

While the ArMs resulting from the covalent and supramolecular anchoring approaches display good to excellent reactivity and selectivity, the dative strategy for which the protein provides one or more amino acid residues to coordinate the metal-containing species is an attractive alternative. In this way, metalloproteins' active site can be efficiently mimicked by taking into account both the first and second coordination spheres.[3] Implanting non-native metallic species within protein scaffolds greatly expands the scope of natural enzymes by allowing the catalysis of abiotic reactions, such as Diels-Alder cycloadditions,[4] C-H bond activation,[5] or cyclopropanation[6].

Engineering of a metal binding site within a protein scaffold can be achieved in several ways. One of which is to take advantage of pre-existing metal coordination sites of metalloproteins and involves metal ion substitution or metal cofactor replacement.[7] Regarding metal ion substitution, this approach has been employed on the zinc enzymes carboxypeptidase A[8] and carbonic anhydrase.[9] Two prerequisites are the easy production of the apoprotein and its sufficient stability. Another rational strategy is to engineer a metal coordination site within a non-metallated protein scaffold[10] or to make use of latent metal binding sites in protein scaffolds.[11] Alternatively, metal binding sites can be created by introduction of unnatural aminoacids *via* genetic engineering.[12] A more serendipitous approach is to make use of the coordination ability of proteins to bind catalytically active metal centres. This approach has been employed with variable success on a small set of protein scaffolds (albumin,[13] apoferritin,[14] lysozyme[15] and streptavidin[16]) and transition metal complexes (Os, Pd, Rh, Mn, Fe, Ru and V). The best results in terms of enantioselectivity were obtained with albumin- and streptavidin-osmium tetroxide hybrids that catalysed the *cis*-dihydroxylation of α-methylstyrene with up to 68%[13a] and 95%[16a] *ee*, respectively.

Asymmetric transfer hydrogenation (ATH) of ketones and imines is a powerful strategy to produce chiral alcohols and amines in a safe, inexpensive and environmentally benign way. Many half-sandwich complexes of Ru^{II}, Rh^{III} and Ir^{III} with phosphorous or nitrogen donor ligands catalyse these reactions in aqueous medium using formate as hydrogen source.[17] Occasionally, peptides have been used as ligands too. For instance, mixtures of dipeptide-like ligands and *p*-cymene dichloro-bridged $ruthenium^{II}$ dimer catalyse the ATH of aryl ketones in isopropanol as hydrogen donor with excellent *ee* values.[18] Along the same line, mixtures of *tris*-aqua complex $[Ir(Cp^*)(H_2O)_3]^{2+}$ and tripeptides such as Gly-Gly-Phe catalyse

This article is protected by copyright. All rights reserved.

Accepted Manuscript

the transfer hydrogenation of a range of ketones in aqueous medium with formate as hydrogen donor with high turnover frequencies (TOFs) but no asymmetric induction was observed.[19] Artificial transfer hydrogenases resulting from the supramolecular assembling of half-sandwich Ru, Rh and Ir complexes to (strept)avidin[20] and carbonic anhydrase[21] have also been shown to catalyse the ATH of ketones and imines with very good efficiency.

Our group has also contributed to the field of ArMs by designing transfer hydrogenases resulting from (i) covalent anchoring of achiral half-sandwich Ru^{II} and Rh^{III} diimine complexes to papain[22] or (ii) supramolecular assembling of related complexes to bovine beta-lactoglobulin (βLG).[23] The latter approach took advantage of the strong affinity of fatty acids for βLG allowing the most efficient construct to catalyse the ATH of the benchmark substrate 2,2,2-trifluoroacetophenone (TFACP) with 59 % conversion and 32% *ee* in 72 h. Presently, the same protein host βLG along with hen egg white lysozyme (HEWL) were used to build up hybrid metalloproteins by the dative anchoring approach. The resulting constructs were shown to display transfer hydrogenase activity on a range of aromatic ketones including TFACP. The most efficient ArM afforded full conversion of TFACP in ca. 12 h with 86% *ee*. This achievement compares favourably with our previous results with βLG and papain as protein hosts.

RESULTS AND DISCUSSION

Preparation and characterisation of metallated beta-lactoglobulin

Prior to metalloprotein assembling, aqueous suspensions of the dimeric complexes $[M(arene)(\mu\text{-}Cl)Cl]_2$ (M = Ru^{II}, arene = *p*-cymene (*p*-cym), benzene (benz) or mesitylene (mes); M = Rh^{III} or Ir^{III}, arene = Cp*, Fig. 1) in water were heated to 50°C for a few minutes. Such a treatment applied to the Ru(benz) dimer in D_2O has been previously shown to afford a mixture of monomeric aqua complexes $[Ru(benz)(D_2O)Cl_2]$, $[Ru(benz)(D_2O)_2Cl]^+$ and $[Ru(benz)(D_2O)_3]^{2+}$ in proportion 8:28:5 as determined by ^1H NMR analysis.[24] This finding has been reproduced in our hands (Fig. S7A).

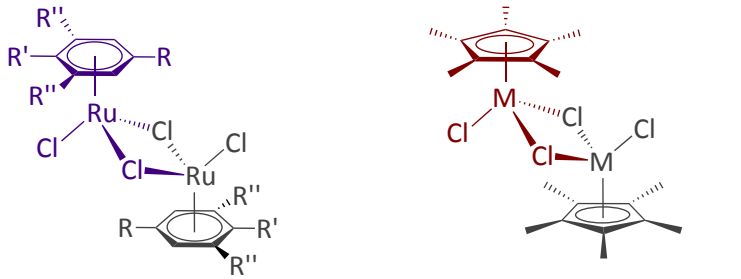

$[Ru(h^6\text{-benz})(m\text{-}Cl)Cl]_2$ R,R',R''H

$[Ru(h^6\text{-}p\text{-cym})(m\text{-}Cl)Cl]_2$ RMe;R'Pr;R''H

$[Ru(h^6\text{-mes})(m\text{-}Cl)Cl]_2$ R,R''Me;R'H

$[Rh(m\text{-}Cl)(h^5\text{-Cp*})Cl]_2$ MRh^{III}

$[Ir(m\text{-}Cl)(h^5\text{-Cp*})Cl]_2$ MIr^{III}

Figure 1. Dimeric half-sandwich Ru^{II}, Rh^{III} and Ir^{III} complexes used as precursors in the catalysis of (A)TH of aromatic ketones.

Then, beta-lactoglobulin was incubated with hydrolysed Ru(benz) at an initial protein/Ru ratio of 1:3 or 1:6 and submitted to gel desalting to separate the protein from unbound

This article is protected by copyright. All rights reserved.

Accepted Manuscript

Ru(benz). The purified metallated protein was submitted to ICP-EOS analysis to determine the Ru concentration (Fig. S1). This together with protein concentration determination at 280 nm, afforded a Ru/βLG of 1.1 (when the initial Ru/βLG ratio was 3:1) and 1.6 (when the initial ratio was 6:1).

The same experiment was performed at an initial molar ratio of 1:1 with hydrolysed Ru(benz), Ru(*p*-cym), Ru(mes), Rh(Cp*) or Ir(Cp*) and UV-visible spectra of metallated proteins were recorded and compared to the hydrolysed complexes alone (Table 1, Fig. S2). All the metallated protein samples (except the Ir adduct) displayed a broad band between 330 and 400 nm tentatively assigned to a metal-to-ligand-charge-transfer (MLCT) transition of the metallic entity. The absorption maximum of this band was blue-shifted by 11 nm for [Ru(benz)] adduct and by 25 nm for [Ru(*p*-cym)] adduct compared to the corresponding hydrolysed metal complex alone. These shifts were undoubtedly assignable to a change of the coordination sphere around the metal upon reaction with the protein. To try to understand which amino acid(s) were involved in metal coordination, the Uv-vis spectra of stoichiometric mixtures of complex and (i) imidazole mimicking histidine as putative *N* donor ligand or (ii) methionine as *S* donor ligand were also recorded. Addition of imidazole shifted the MLCT band shifted to the blue by 8 to 15 nm while addition of methionine shifted the MLCT band to the blue by 16 to 25 nm. On the whole, the position of the MLCT band of the biohybrids is close to that of the mixtures of complex with methionine. Nevertheless, it would be presumptuous to assert that methionine is the amino acid involved in metal coordination on the sole basis of absorption spectroscopy.

Table 1. Position of the MLCT band of hydrolysed M(arene), βLG•M(arene) (initial M/βLG = 1:1) and stoichiometric mixtures of M(arene) and imidazole or methionine in water

M	arene	M(arene)		βLG•M(arene)		M(arene)+imidazole		M(arene) + methionine	
		λ_{max} (nm)	ε ($M^{-1}cm^{-1}$)	λ_{max} (nm)	ε ($M^{-1}cm^{-1}$)	λ_{max} (nm)	ε ($M^{-1}cm^{-1}$)	λ_{max} (nm)	ε ($M^{-1}cm^{-1}$)
Ru	benz	394	410	382	630	386	375	378	440
Ru	mes	400	450	378	670	388	420	n.d.	n.d.
Ru	*p*-cym	403	560	378	500	388	460	378	520
Rh	Cp*	378	1700	360	2800	367	1800	356	3000

Addition of hydrolysed Ru(benz) to a solution of βLG in water decreased the intrinsic fluorescence of the protein's two tryptophan residues at 336 nm. Gradual quenching was observed upon addition of complex until saturation was reached at ca. Ru/βLG = 5:1 (Fig. S5). Titration of βLG by hydrolysed Ru(benz) was also monitored by Uv-vis spectroscopy and the difference spectra depicted in Fig. S4 show the appearance of a band centred at ca. 325 nm upon addition of Ru(benz) which is characteristic of the biohybrid. Near Uv CD spectra of mixtures of βLG and hydrolysed Ru(benz) also showed a positive band centred at ca. 320 nm as a result of biohybrid formation (Fig. S4).

Mass spectrometry analysis of metallated βLG

This article is protected by copyright. All rights reserved.

Accepted Manuscript

The isoform A of βLG (βLG-A) was incubated with 0, 1, 2 or 3 mole eq. of hydrolysed Ru(benz) complex in water for 1 h. The mixtures were next analysed by electrospray-high resolution mass spectrometry (ESI-HRMS). The mass spectrum of native βLG-A reveals a charge states distribution from 10+ (*m/z* 1837.36) to 19+ (*m/z* 967.35) and centred around 14+ and 15+, at *m/z* 1225.17 and *m/z* 1312.62, respectively (Fig. 2A).

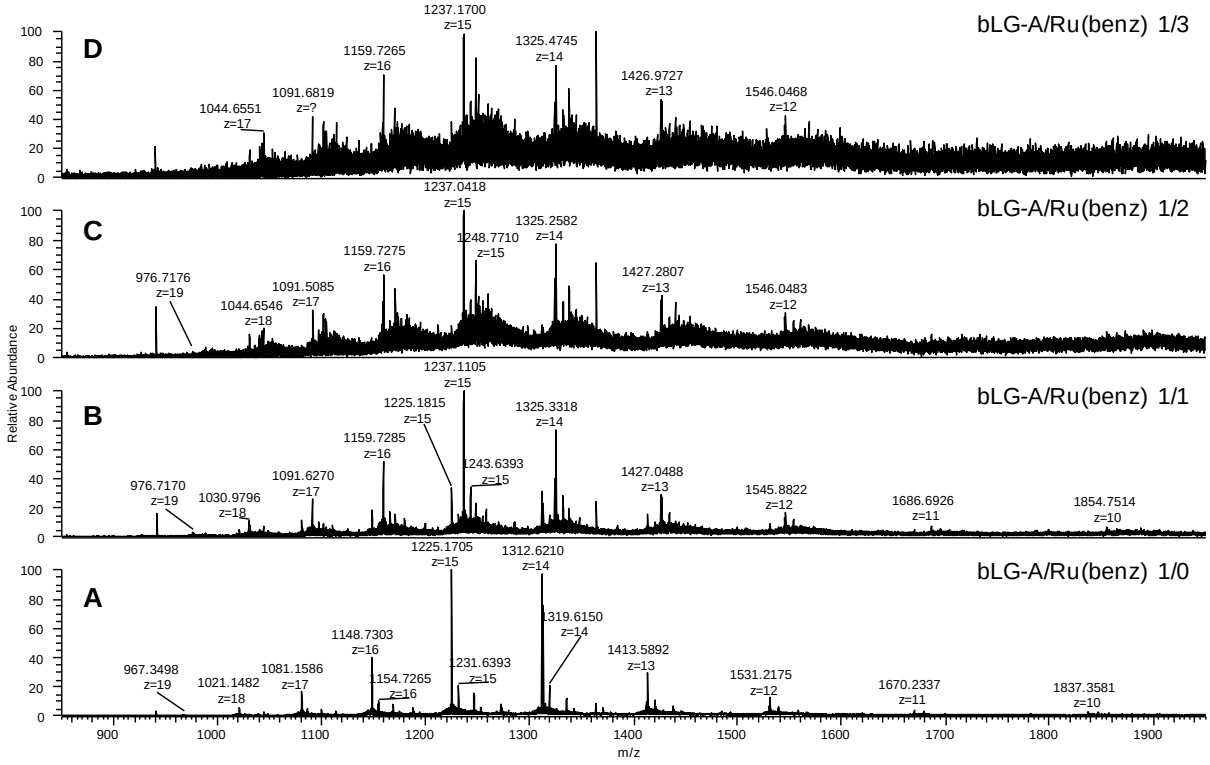

Figure 2. ESI-HRMS mass spectra of βLG-A without Ru(Benz) (A) and resulting from the reaction of 1 (B), 2 (C) or 3 (D) mole eq. hydrolysed Ru(benz) after incubation in water for 1 h at RT.

Increase of Ru(Benz) from 0 to 3 eq. resulted in the progressive formation of metallated βLG-A detected as a metalloprotein with charge states ranging from 10+ (*m/z* 1854.75) to 19+ (*m/z* 977.71) (Fig. 2B-D). To confirm that the exact nature of the metal fragment bound to the protein was a $[Ru(benz)]^{2+}$ entity, a comparison between calculated and experimental isotopic distribution patterns of the most prominent 15+ ion of βLG-A and βLG-A + Ru(benz) was performed (Fig. 3)

Accepted Manuscript

This article is protected by copyright. All rights reserved.

A

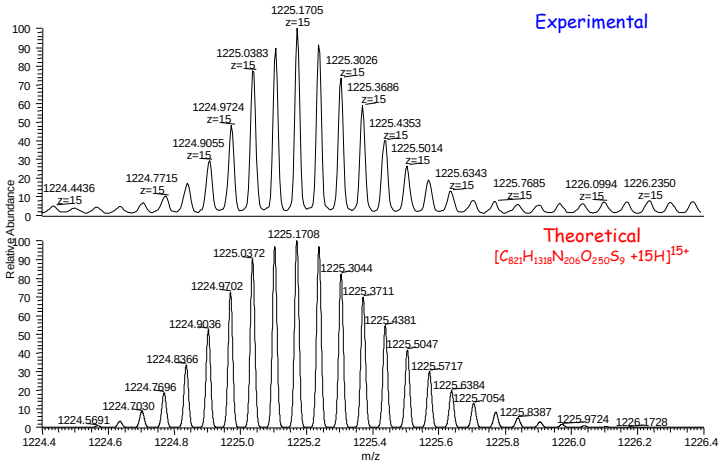

B

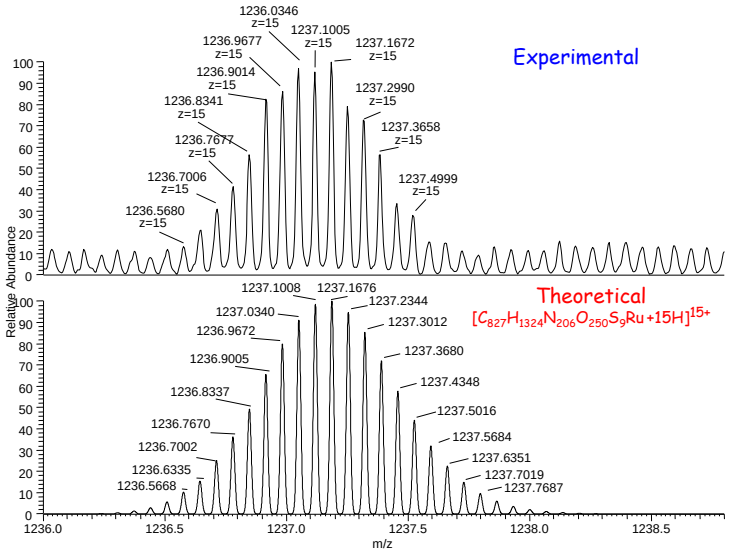

Figure 3. Isotopic distribution of 15+ ion for βLG-A (A) and βLG-A + Ru(benz) (B) with experimental (upper) and calculated (lower) patterns.

Experimental isotopic profiles obtained for βLG-A (Fig. 3A) and βLG-A + Ru(benz) (Fig. 3B) matched very well with the calculated isotopic patterns. As regards βLG-A + 2[Ru(benz)], it was quite difficult to make a straightforward assignment based only on the isotopic pattern due to very low signal and possible resulting truncated distribution (not shown). Furthermore, the aforementioned data i.e. multicharged spectra and isotopic profiles do not give access to both exact masses and sample content. Consequently, to get further pieces of information about the content of βLG-A and various complexes formed, deconvolution and deisotoping steps were achieved (Fig S6). Deconvoluted mass spectrum of βLG-A only (Fig. S6A) showed a major peak at a monoisotopic mass of 18,351.5205 which is in good agreement with the theoretical value of βLG-A (18,351.4234 g.mol^{-1}; 5 ppm). Two other minor species at masses of 18,449.4984 and 18675.6266 (Fig. S6A) were also observed. The former one was assigned to a neutral adduct with phosphoric acid (mass shift of +97.98), as

This article is protected by copyright. All rights reserved.

Accepted Manuscript

described elsewhere for other proteins,[25] and the latter to a typical product of lactose condensation (mass shift of +324.11) consecutively to the Maillard reaction.[26] As regards the spectra corresponding to complexation of βLG-A with Ru(Benz) at 1, 2 and 3 mole eq. (Fig. S6B-D), except for a residual amount of free protein, two prominent additional species appeared in the masses range between 18,529.4977 to 18,529.5314 and 18,707.4466 to 18,707.4488. Taking into account the mass obtained for βLG-A only, these species correspond to two consecutive average mass shifts of 177.95. Such values can certainly be attributed to complexation of βLG-A with 1 and 2 $[Ru(Benz)]^{2+}$. In addition, according to aforementioned values, a good agreement was also obtained with theoretical masses i.e. 18,529.3882 $g.mol^{-1}$ (5^{th} isotope; 5 ppm) and 18,707.3452 $g.mol^{-1}$ (5^{th} isotope; 3 ppm) for βLG-A + one Ru(benz) and βLG-A + two [Ru(benz)], respectively. Assuming that all species exhibit a similar ESI response factor, relative quantification of various species yielded ratios of native βLG-A/Ru bound forms of 21/79 and 10/90, with 1 and 2 mole eq. hydrolysed Ru(benz), respectively. Further increase to 3 mole eq. hydrolysed Ru(benz) yielded a similar proportion of native βLG-A and Ru bound proteins (13/87). In detail, among the ruthenated protein forms, the mono-metallated one was in all cases the most prominent with 61, 51 and 65% content for Ru(benz)/βLG-A ratios of 1:1, 2:1 and 3:1, respectively. The average number of Ru atoms bound per βLG calculated from the proportion of native βLG-A, monoruthenated βLG-A and diruthenated βLG-A equalled 1.09 for the initial Ru(benz)/βLG ratio of 3:1, in excellent agreement with the ICP-OES data given above (1.1).

All the spectroscopic data obtained by different techniques point out to the formation of organometallic biohybrids resulting from the coordination of beta-lactoglobulin to the metal centre.

Transfer hydrogenation of TFACP catalysed by metallated βLG

First, the ATH of TFACP in the presence of metallated βLG resulting from the reaction with 1 eq. of hydrolysed half-sandwich complexes (βLG•M(arene) and sodium formate as hydrogen donor was tested (Scheme 1). In parallel, control experiments were carried out with the hydrolysed complexes alone. Conversion and enantiomeric excess (*ee*) were determined by chiral HPLC of the reaction mixtures after 33 h (Fig. 4).

Scheme 1. (Asymmetric) Transfer Hydrogenation of TFACP

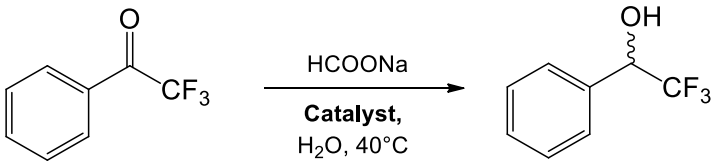

Figure 4. (A)TH of TFACP (5 mM) catalysed by βLG•M(arene)$_1$ or hydrolysed M(arene) (0.1 mM). Conditions: [HCOONa] = 1 M, pH = 7.5, T = 40°C. Top: conversion and *ee* measured after 33 h; bottom: turnover frequency (TOF)

This article is protected by copyright. All rights reserved.

Accepted Manuscript

10.1002/ejic.201701359

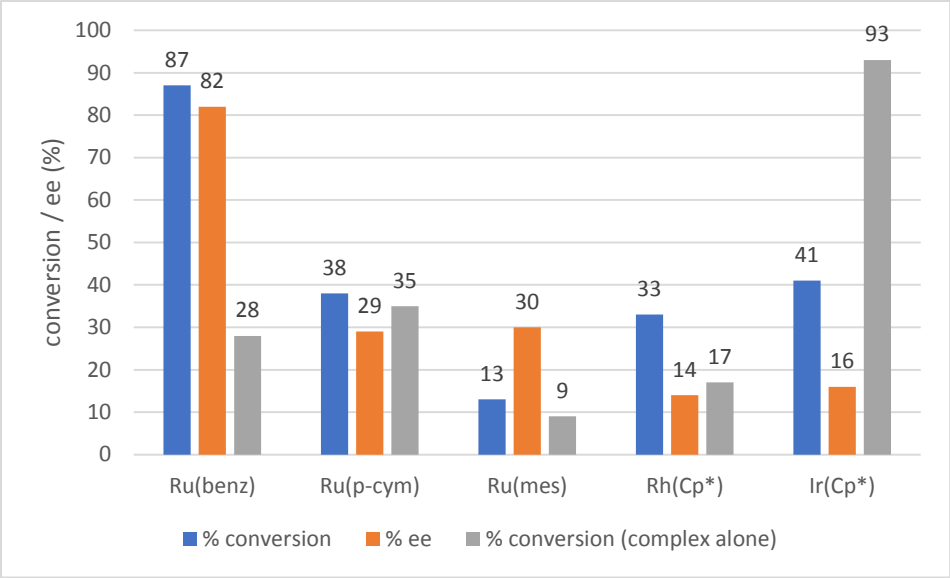

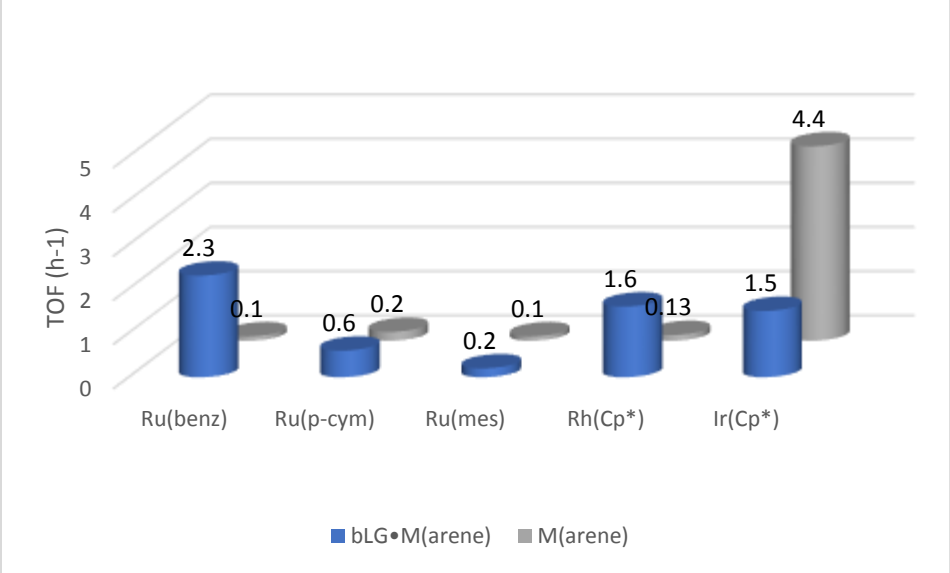

Conversion of TFACP catalysed by the half-sandwich metal complexes alone clearly depended on the metal and, in the Ru series, on the nature of the ancillary aromatic ligand. The Ir complex alone was the most active of the series since full conversion was observed after 33h in good agreement with Ogo and Watanabe's findings for $[Ir(Cp^*)(H_2O)_3]^{2+}$.[27] In accordance, our evaluations let to rank the catalytic activity of complexes alone in the following order: Ir(Cp*) >> Ru(*p*-cym) > Ru(benz) > Rh(Cp*) > Ru(mes). In the case of the Ru(benz) complex, the mechanism of transfer hydrogenation involved the transient formation of a Ru-H species as observed by ^{1}H NMR spectroscopy by the presence of a singlet at -7.03 ppm (Fig. S7) in the range of previously reported (arene)(L^L)Ru-H species (between -5 and -8 ppm depending on the L^L ligand).[28] As expected, the corresponding alcohol was obtained as a racemic mixture in all cases where complexes were used alone.

On the other hand, all the metalloprotein hybrids were also found to catalyse the ATH of TFACP with conversions ranging from 13% for the least active biocatalyst βLG•Ru(mes) to 87% for the most active biocatalyst βLG•Ru(benz). Surprisingly a completely different

This article is protected by copyright. All rights reserved.

Accepted Manuscript

ranking was established for the hybrid catalysts in comparison to that of the complexes alone, i.e. βLG•Ru(benz) >> βLG•Ir(Cp*) ~ βLG•Ru(*p*-cym) > βLG•Rh(Cp*) > βLG•Ru(mes). Moreover, the (*R*)-enantiomer of α-(trifluoromethyl)benzyl alcohol was obtained preferentially with all the metallated βLG; with *ee* ranging from 15% for the least selective catalyst βLG•Rh(Cp*) to 82% for the most selective catalyst βLG•Ru(benz). Let us notice that both the Rh and the Ir hybrids gave the same *ee*, while βLG•Ru(*p*-cym) gave the same *ee* as βLG•Ru(mes). This similarity might be due to identical coordination sites for both pairs of complexes.

The TOF representing the initial reaction rate was then calculated at 1 h reaction time for all the βLG•M(arene) and compared to that afforded by the complexes alone (Fig. 4, bottom). The rate of TH of TFACP was markedly enhanced by coordination of βLG to the Ru(benz) complex (enhancement factor = 23). Protein coordination to the two other Ru complexes and the Rh one enhanced the rate of reaction to a lesser extent (enhancement factor < 3 for Ru and 12 for Rh). Interestingly, βLG coordination decreased the activity of the iridium complex by a factor of 3.

Next, βLG was treated with Ru(benz) at 1:3 or 1:6 ratio as described above. The resulting biohybrids were tested in the ATH of TFACP under standard conditions. The concentrations of ketone and alcohol in the reaction mixtures were monitored overtime by chiral HPLC. Conversion plots are shown in Fig. 5 and table 2 gathers the related kinetic data.

Figure 5. Time course of ATH of TFACP (5 mM) catalysed by βLG•Ru(benz) (Ru/bLG = 1:1, 3:1 or 6:1). Conditions: 2 mol% cat, [HCOONa] = 1 M, pH = 7.5, T = 40°C, V = 1 mL.

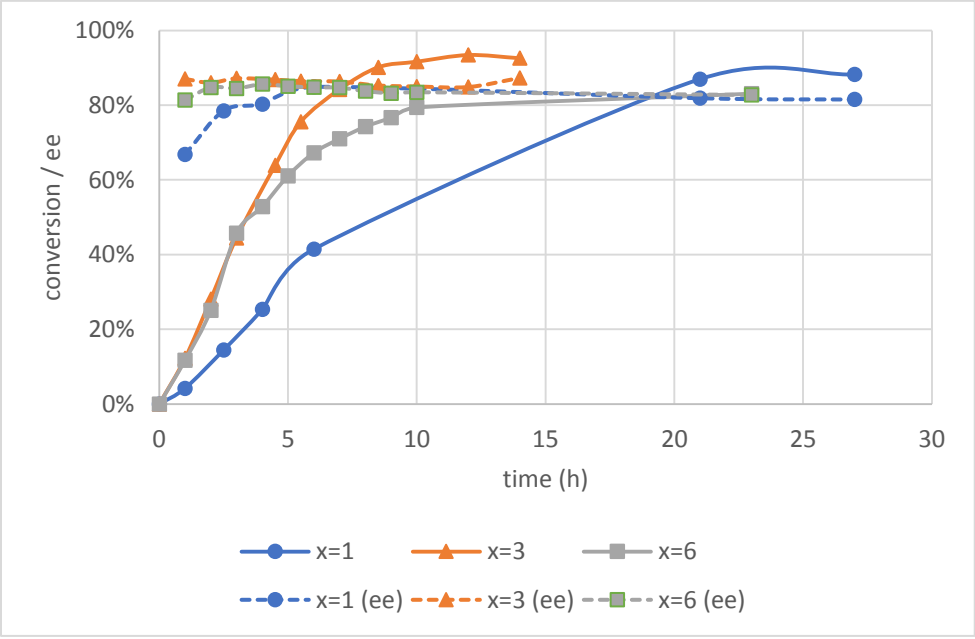

Accepted Manuscript

This article is protected by copyright. All rights reserved.

Table 2. (A)TH of TFACP. TOF, conversions and *ee* with Ru(benz) derived catalysts. Conditions: [TFACP] = 5 mM, 2 mol% βLG, [HCOONa] = 1 M, pH 7.5, 40°C, v=1 ml

entry	Catalyst	βLG/Ru(benz) ratio	k_{obs} (h^{-1})	TOF (h^{-1})	Conversion (%) and time (h)	*ee* (%)
1	βLG•Ru(benz)	1:1	0.086±0.015	2.3	87 (21)	82 (*R*)
2	βLG•Ru(benz)	1:3	0.23±0.03	6.1	93 (12)	87 (*R*)
3	βLG•Ru(benz)	1:6	0.25±0.02	6.7	79 (10)	83 (*R*)
4	βLG + Ru(benz)	1:3	n.d.	3.2	99 (05)	78 (*R*)
5	βLG-DMPC + Ru(benz)	1:3	n.d.	0.8	96 (25)	69 (*R*)
6	imidazole + Ru(benz)[a]	1:1	0.083±0.015	1.2	94 (25)	0

[a] [imidazole] = [Ru(benz)] = 0.3 mM

Nearly complete conversion of TFACP was observed with the three biocatalysts. The initial TOF (Table 2) ranged from 2.3 h^{-1} for βLG/Ru(benz) = 1:1 to 6.7 h^{-1} for βLG/Ru(benz) = 1:6. The rate constant of reaction k_{obs} (calculated assuming first order kinetics) followed the same trend. The TOF afforded by βLG/Ru(benz) = 1:3 was ca. three times that afforded by βLG/Ru(benz).= 1:1. In contrast, the TOF afforded by βLG/Ru(benz) = 1:6 was only slightly higher than that of βLG/Ru(benz) = 1:3, which is in line with the similar final Ru/protein ratio of both samples (see above). All three biocatalysts afforded constant *ee* values slightly above 80% over the time range which indicates that they remained stable all along.

A catalytic run was performed with a crude mixture of βLG and Ru(benz) at ratio of 1:3 in the same experimental condition (Table 2, entry 4). Conversion reached 99% in 5h and the *ee* of the *sec*-alcohol was 78%. The presence of metal complex alone in the reaction mixture only very slightly altered the overall selectivity. This finding can be explained by the very poor reactivity of the Ru(benz) complex by itself compared to the protein coordinated form. Time course of ATH of TFACP in the presence of mixture of βLG and Ru(benz) at molar ratio of 1:5 and sodium formate was also monitored by ^{1}H NMR in D_2O (Fig. S8). Signals of the aromatic protons of TFACP progressively decreased, while a multiplet and a well resolved quadruplet belonging to the *sec*-alcohol product gradually appeared. The evolution of the ^{1}H NMR spectrum of the reaction is consistent with consumption of ketone and formation of alcohol. A singlet at 5.56 ppm tentatively assigned to the protons of the benzene ligand of a [Ru-formato] adduct was simultaneously seen to decrease until complete ketone conversion.

Substrate scope

The ArM formed by simply mixing βLG and Ru(benz) at ratio of 1:3 was applied to the ATH of other aromatic ketones. All the catalytic runs were performed at 1 mol% βLG (3 mol% [Ru(benz)]). Conversion and enantioselectivity were measured by chiral GC analysis of the reaction mixtures after 40 h at 40°C (Table 3).

Accepted Manuscript

This article is protected by copyright. All rights reserved.

10.1002/ejic.201701359

Table 3. ATH of various aryl ketones in water.[a]

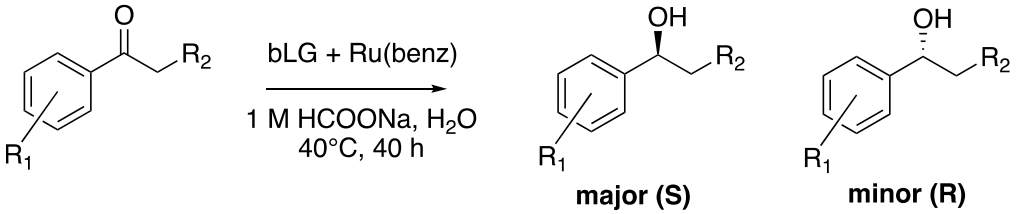

R_1	R_2	Conversion (%)	*ee* (%)
H	H	63	11
H	Me	81	23
***o*-Me**	H	n.d.	55
***m*-Me**	H	n.d.	17
***p*-Me**	H	82	12
***o*-MeO**	H	55	41
***m*-MeO**	H	n.d.	6
***o*-Br**	H	n.d.	74
***m*-Br**	H	n.d.	15
***o*-NO_2**	H	52	75
***o*-CF_3**	H	77	28
***o*-F**	H	80	73

[a] [substrate] = 10 mM, [βLG] = 0.1 mM, [Ru(benz)] = 0.3 mM, [HCOONa] = 1 M, pH = 7.5; n.d: not determined

The mixture of βLG and Ru(benz) was also able to catalyse the ATH of non-activated aryl ketones in aqueous medium. The presence of substituents in *ortho* position of the methyl ketone group induced significant stereoselectivity, up to 75% *ee*, while substituents at the two other positions had nearly no effect. Interestingly, the (*S*)-enantiomer was obtained preferentially for all the tested ketones (and the (*R*)-enantiomer for the hydrogenation product of TFACP), indicating that the nucleophilic hydride attack always occurred at the same face of the substrate. Indeed, the R/S formalism is based on the Cahn, Ingold and Prelog priority rules that place the CF_3 group above the Ph group and the Ph group above the CH_3 group.

Transfer hydrogenation of TFACP catalysed by metallated HEWL

It has been recently shown that association of Ru(benz) and cross-linked crystals of HEWL catalyse the TH of acetophenone derivatives with variable selectivity.[15] Thus, as a preliminary screening, we examined the ability of crude mixtures of HEWL and hydrolysed M(arene) complexes (M = Ru, arene = benz or *p*-cym; M = Rh or Ir, L = Cp*) at mole ratio 1:1 to catalyse the ATH of TFACP. For comparison, the conversion of TFACP was measured in the presence of the complexes alone (Fig. 6).

Accepted Manuscript

This article is protected by copyright. All rights reserved.

10.1002/ejic.201701359

Figure 6. ATH of TFACP (10 mM) catalysed by HEWL + M(arene) (0.2 mM) or M(arene) (0.2 mM). Conditions: [HCOONa] = 1 M, pH = 7.5, T = 40°C, t = 9 h

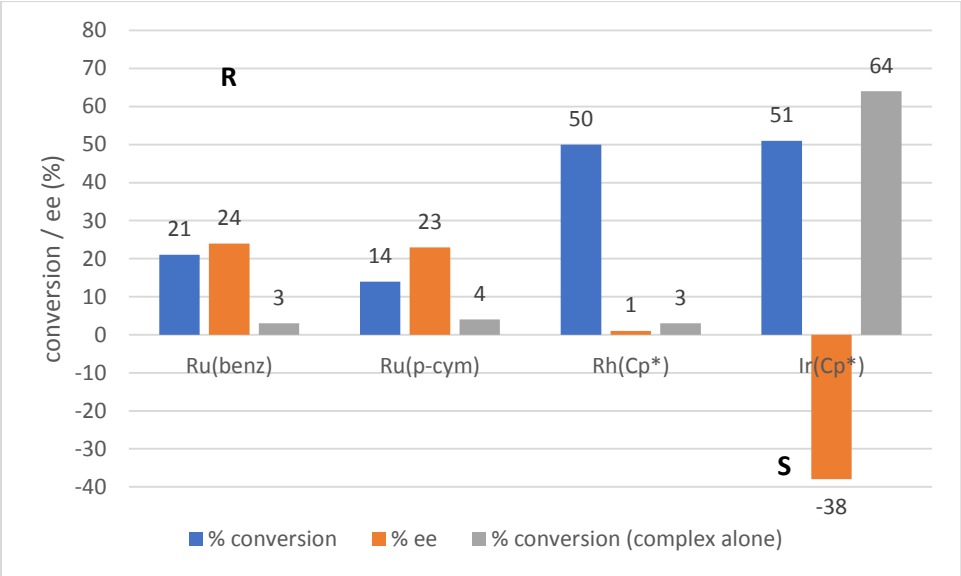

All the mixtures were able to catalyse the ATH of TFACP with the following ranking HEWL+Ir(Cp*) ~ HEWL+Rh(Cp*) > HEWL+Ru(benz) > HEWL+Ru(*p*-cym). This is dramatically different from the ranking established for the βLG biohybrids. The presence of HEWL in the reaction mixture markedly enhanced the activity of the metal complexes except again for Ir(Cp*) for which a slight decrease of the conversion was observed in the presence of HEWL. This finding and asymmetric induction observed for 3 of the 4 mixtures is in agreement with protein coordination to the metal centre. Enantiomeric excesses were different from those previously measured with the βLG biohybrids and, quite surprisingly, the mixture of HEWL and Ir(Cp*) afforded preferentially the (*S*)-enantiomer of α-(trifluoromethyl)benzyl alcohol, whereas the mixtures of HEWL and the Ru complexes gave the (*R*)-isomer as before. The rather poor selectivity of the HEWL + Ru(benz) mixture is in line with previously reported results on other acetophenone derivatives.[15]

Therefore we synthesized HEWL•Ir(Cp*) biohybrids by reacting HEWL and hydrolysed Ir(Cp*) at initial ratios of 1:1, 1:5 or 1:10. After purification by gel filtration, time course of ATH of TFACP in the presence of the metallated proteins HEWL•Ir(Cp*) (HEWL/Ir ratios = 1:1, 1:5 or 1:10) was monitored by chiral HPLC. As seen in Fig. 7 and Table 4, the rate of conversion and enantiomeric excess depended on the initial HEWL/Ir ratio with the fastest rate and the highest *ee* (43%) measured for ratio 1: 10. Moreover, the enantiomeric excess tended to decrease with time, the magnitude of this decrease heightened with reaction time. This trend was undoubtedly related to an evolution of the nature of the catalytic species during the time course of the reaction; one possible change may be related to decomplexation of the protein ligand. Quite unexpectedly, the catalytic performances of HEWL•Ir(Cp*) and HEWL+Ir(Cp*) (at 1:1 ratio) differed significantly since the mixture of HEWL and Ir(Cp)* was a more selective catalyst than HEWL•Ir(Cp*)$_1$ (38% vs. 7 % ee). Correlatively, the gel filtration step decreased the selectivity of the hybrid catalyst. We can reasonably assume that HEWL

This article is protected by copyright. All rights reserved.

Accepted Manuscript

contains several binding sites for Ir(Cp*), each one of these having its own binding constant and the ability to afford a specific enantioselectivity. Gel filtration may have induced dissociation of the iridium complex from the weakest protein binding site(s) which may also have been those providing the highest selectivity in the ATH of TFACP.

Figure 7. Time course of ATH of TFACP (5 mM) catalysed by HEWL•Ir(Cp*) (HEWL/Ir ratio = 1:1, 1:5 or 1:10). Conditions: 2 mol% cat, 1 M HCOONa in HEPES buffer pH 7.8, T = 40°C, v=1 ml.

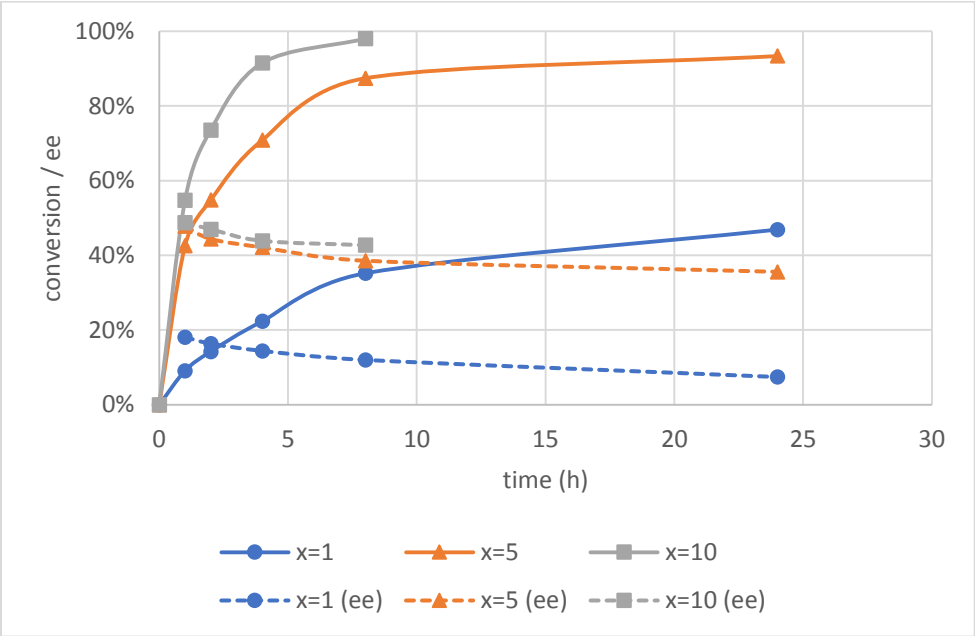

Table 4. (A)TH of TFACP, TOF, conversions and *ee* with Ir(Cp*) derived catalysts. Conditions: [TFACP] = 5 mM, 2 mol% HEWL, 1 M HCOONa in HEPES buffer pH = 7.8, T = 40°C, V = 1 mL.

Catalyst	HEWL/Ir ratio	k_{obs} (h^{-1})	TOF (h^{-1})	Conversion (%) and time (h)	*ee* (%)
HEWL•Ir(Cp*)	1:1	0.16±0.01	3.7	47 (24)	7 (*S*)
HEWL•Ir(Cp*)	1:5	0.48±0.09	18.6	93 (24)	36 (*S*)
HEWL•Ir(Cp*)	1:10	0.78±0.07	24.4	98 (8)	43 (*S*)
Ir(Cp*)[a]	-	0.11±0.02	4.4	93 (14)	0
HEWL+Ir(Cp*)[b]	1:1	n.d.	3.2	51 (9)	38 (*S*)

[a] [Ir(Cp*)]=0.1 mM, 1 M HCOONa pH 7.5; [b] [HEWL]=[Ir(Cp*)]=0.2 mM, [TFACP]=10 mM, [HCOONa]=1 M, pH 7.5

Tentative determination of ruthenium binding site(s) on beta-lactoglobulin

A survey of the literature dealing with the interaction of half-sandwich Ru^{II} complexes with proteins may give clues as to their preferential protein binding sites. The Ru(*p*-cym) and the Ru(benz) complexes were shown to bind to crystallized HEWL at its sole His residue (His15) with a second minor binding site at Asp101.[15,29] This behaviour was explained by the favourable local environment around His15 and its good accessibility in the crystal state. Moreover, His15 is surrounded by a cluster of residues creating a pocket of the right size for

This article is protected by copyright. All rights reserved.

Accepted Manuscript

the complex to fit in. When the multimeric protein apoferritin was treated with a large excess of $[Ru(p\text{-cym})Cl_2]_2$, three main binding sites were identified by X-ray crystallography: (i) one involving two His and one Glu; (ii) another one involving one Glu, one Asp and one Cys and (iii) the last one involving one Cys and one His.[14b] The anticancer complex RAPTA-C ($[Ru(p\text{-cym})(pta)Cl_2]$) bound preferentially to His33 of cytochrome c.[30] Another anticancer complex namely, $[Ru(p\text{-cym})(en)Cl]PF_6$ (en = ethylenediamine), bound to human albumin via coordination of its sole free cysteine residue (Cys34) as well as three accessible histidines and one methionine.[31] The same complex was found to bind to three *S*-donor cysteine residues of human glutathione-*S*-transferase.[32]

Beta-lactoglobulin offers several putative coordination sites (*O*, *N* and *S* donor ligands) for the Ru(benz) complex. Considering that the main product of hydrolysis of the ruthenium dimer is the *bis*-aqua monomeric adduct $[Ru(benz)(H_2O)_2Cl]^+$, there should be at least two positions available for coordination of βLG that may act as a monodentate or a bidentate ligand. Beta-LG contains two histidines (His146 and His161), one free cysteine (Cys121), two methionines (Met7 and Met145), 15 glutamates and 11 aspartates. The two Met are poorly accessible and Cys121 is completely inaccessible (located at the outer surface of the beta-barrel on strand H under the alpha-helix).[33] From the calculation of surface accessibilities, only one of the two histidines, namely His146, appears to be surface-exposed. Indeed, assay of βLG's histidines with diethyl pyrocarbonate (DEPC) according to Miles[34] gave a number of modified histidines equal to one. However, at neutral pH, βLG exists as a dimer with a dissociation constant in the micromolar range.[35] X-ray crystallographic studies showed that dimer association occurs via a network of hydrogen bonds between the β-strands I (residues 146-152) of both monomers that assemble in a head to tail fashion.[36] The 3D-structure of βLG dimer at pH 7.1 (PDB file 1BSY) is depicted in the supplementary information section (Fig. S9). It clearly shows that His146 is positioned in a somewhat narrow cavity at the edge of the interfacial region between the two monomers with only the *N*ε accessible to solvent.

To check whether His146 was involved in the coordination of Ru(benz), βLG was treated with excess dimethylpyrocarbonate (DMPC)[37] which has a similar reactivity as DEPC. *N*-methoxycarbonylation of imidazole ring is assumed to make the remaining nitrogen of histidine a poorer ligand and thus potentially inhibit metal coordination.[9b] After gel filtration to remove excess DMPC, the βLG-DMPC conjugate was mixed with hydrolysed Ru(benz) at Ru/βLG ratio of 3:1 with no further purification. Conversion of TFACP and enantiomeric excess were measured at different time points (Fig. 8 and table 2). Pre-treatment of βLG with DMPC led to a dramatic decrease of the rate of ATH as compared to untreated βLG (TOF = 0.8 h^{-1} vs. 3.2 h^{-1}). The enantiomeric excess was also significantly affected, ranging from 34% to 64% during the reaction. This different behaviour of βLG-DMPC provided a solid clue as to the involvement of His146 in ruthenium coordination. However, since some enantioselectivity was still observed, His146 is probably not the sole residue to be involved in ruthenium coordination, which agrees well with the presence of a doubly ruthenated protein complex identified by ESI-HRMS. Another hypothesis is that

This article is protected by copyright. All rights reserved.

Accepted Manuscript

gradual increase of the *ee* may be due to the progressive removal of the –C(O)OMe group during catalysis that enables His146 to coordinate back to Ru(benz). The stability of *N*-(alkoxycarbonyl)imidazole is known to be pH-dependent and dealkoxycarbonylation is readily achieved by treatment with NH_2OH at neutral pH.[34] Such a reaction may have also occurred in the presence of 1 M HCOONa at 40°C.

Figure 8. Time course of ATH of TFACP (5 mM) catalysed by βLG (0.1 mM) + Ru(benz) (0.3 mM) or βLG-DMPC (0.1 mM) + Ru(benz) (0.3 mM).

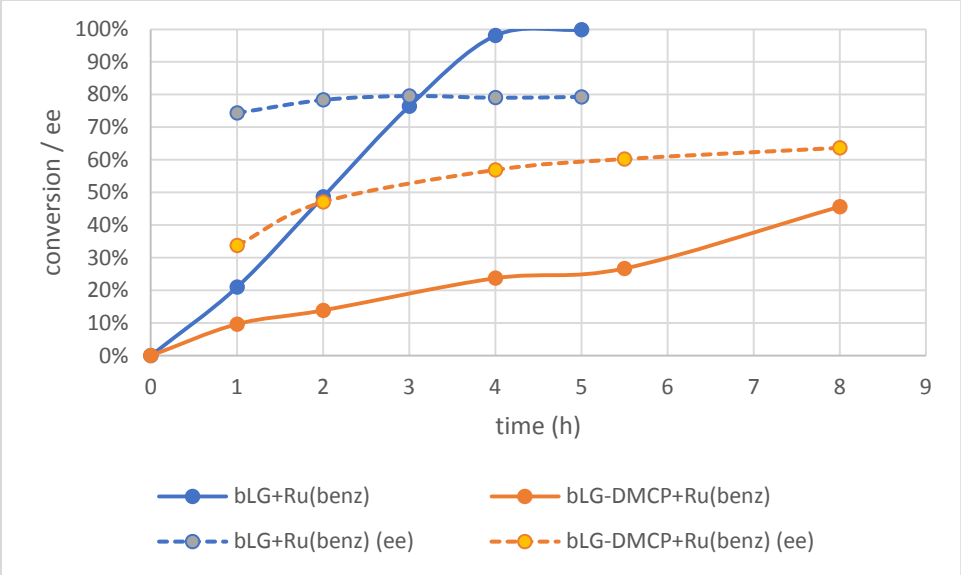

Aiming at identifying amino acid residues or at least the part of sequence of βLG-A involved in the coordination to Ru(benz), two MS-based approaches i.e. MALDI-TOF and ESI-MS/MS were attempted. No ruthenated peptides were detected by MALDI-TOF analysis performed after disulphide bond reduction by dithiotreitol (DTT) and denaturation steps followed by trypsin digestion (data not shown). It appeared that the ruthenated protein did not withstand the conditions used for this type of analysis which could be due to reductive/denaturing treatment as well as too high disrupting energy dispensed by laser as observed elsewhere for small proteins (insulin–platinum complex).[38] Such results may reflect the relative weakness of the bond(s) between the protein and the metal ion to be expected if the protein coordinates to the ruthenium centre in a monodentate fashion.[39] Such an issue has been recently pointed out by Michelucci and coll.[40] Moreover, attempts to crystallize ruthenated βLG-A or to introduce the metallic species in βLG single crystals by diffusion were also unsuccessful (data not shown).

To overcome the drawback of laser used for ionization process, ESI-top-down analysis was performed aiming at MS/MS sequencing of ions of the whole protein. Such a strategy has been successfully applied to determine the copper binding sites of chloroplastic protein,[41] as well as the iridium[42] and the platinum[43] binding sites of calmodulin. The binding sites of half-sandwich ruthenium(II) complexes on angiotensin and bombesin[44] were investigated by the same technique as well as platinum binding sites on copper metallo-chaperone,[45] insulin,[46] and ubiquitin[47].

This article is protected by copyright. All rights reserved.

Accepted Manuscript

Thus, to favour residues accessibility upon fragmentation, a reduction step of βLG-A was carried out by DTT (0.5 mM, 1 h at 37°C). More intense, but similar multicharged ions were obtained before (Fig. S10A) and after treatment of native βLG-A (Fig. S10B), since cleavage of the two disulphide bridges yields a neutral mass shift of only +4.0312. However, similar treatment on βLG-A/Ru(Benz) 1:1 yielded the complete dissociation of the Ru(benz) moiety (Fig. S10C-D). Modifications of reduction conditions, i.e. temperature and/or incubation time, from 37°C to room temperature and 1h to 2h, respectively, led to similar results (Fig S10D-E). Such results unambiguously demonstrated that βLG-A/Ru(benz) complex was sensitive to a reduction step, and that the proximity of the disulphide bridges could be essential to maintain a minimal structure allowing the ligation of Ru(benz) as observed for the small chloroplastic protein with copper.[41] Herein, loss of Ru(benz) can be due to a direct action of DTT on Ru(benz) and/or protein unfolding, resulting in disulphide bridge cleavage, and inducing modifications of the coordination sphere. MS/MS experiments on the 19+ ion of βLG-A without (*m/z* 967.50, Fig. S11A) or with Ru(Benz) (*m/z* 977.50, Fig. S11B), revealed abundant and numerous fragments with some of them exhibiting a clear neutral mass shift of +177.95 when comparing native βLG-A to βLG-A metallated with Ru(Benz). After identification of these fragments, such results give unambiguous evidences that the Ru(benz) entity was located in the *N*-terminal region of the protein. However, as no reduction step was possible (see above) without triggering ruthenium dissociation, it was not possible to precisely identify the residues(s) involved in metal coordination. Moreover, it must be kept in mind that previous literature examples of mapping of metalation sites were performed on proteins exhibiting shorter sequence (<100 amino acids, except calmodulin with 158 residues) and lacking disulphide bridges. Clearly, ruthenated βLG-A, because of its folding, its larger size and its two disulphide bridges appeared to be more case sensitive to study.

CONCLUSIONS

In summary, association of organometallic [M(arene)] entities to the proteins βLG and HEWL afforded artificial metalloenzymes with transfer hydrogenase activity on various aromatic ketones. The most active, stereoselective and stable hybrid catalyst was obtained with M = Ru, arene = benzene and βLG as protein host. Additional experiments shed light on the nature of the hybrid species. Both mass spectrometric analysis and ICP-OES disclosed that treatment of βLG with $[Ru(benz)]^{2+}$ gave a mixture of mono- and di-ruthenated adducts. Interestingly, the crude hybrid catalyst was nearly as effective as the purified one. The hybrid catalysts derived from HEWL were less selective, with the iridium adduct providing an opposite stereoselectivity. Moreover, the HEWL•Ir(Cp*) adduct appeared to be unstable in our conditions of transfer hydrogenation; as deduced from the progressive decrease of enantiomeric excess recorded in the course of the reaction. Eventually, a top down mass spectrometry approach using collision-induced dissociation fragmentation enabled to narrow the ruthenium binding sites on beta-lactoglobulin to the *N*-terminal region. Finally, our approach provided new efficient metalloenzymes with rather good catalytic properties.

This article is protected by copyright. All rights reserved.

Accepted Manuscript

These might be further improved by genetic optimisation of the protein host. Computational methods[48] along with electrochemical studies could be undertaken to get further insight on the binding site(s) and stability of metallated protein adducts with organometallic half-sandwich metal complexes.

Experimental section

General methods

Dichloro (arene) ruthenium, rhodium and iridium dimers and dithiothreitol (DTT) were purchased from Strem chemicals or Sigma-Aldrich (Saint-Quentin-Fallavier, France). βLG (mixture of both isoforms 85% purity, or isoform A), hen egg white lysozyme, diethylpyrocarbonate (DEPC), dimethylpyrocarbonate (DMPC) and sodium formate were purchased from Sigma-Aldrich and used as received. ^{1}H NMR spectra were recorded either on 300 or 400 MHz spectrometers (Bruker). Chemical shifts are quoted in parts per million (ppm) and referenced to residual H signal of HOD (4.78 ppm).

Synthesis of βLG•M(arene)

A suspension of dichloro (arene) metal dimer in water was heated to ca. 50°C for a few minutes until complete dissolution. A solution of βLG (172 µM in water, 2 mL) was mixed with a solution of hydrolysed M(arene) (5 mM metal in water) to make a M/ βLG ratio of 1:1, 3:1 or 6:1. After ca. 1h at RT, the mixture was submitted to gel filtration on a prepacked column (Pierce dextran desalting column, 10 mL, Thermo-scientific) using water as eluent. Twelve 1-mL fractions were collected manually and analysed at 280 nm. The fractions containing the protein were pooled and the solution concentrated by centrifugal ultra-filtration. Protein concentration was assayed at 280 nm taking ε = 17,600 $M^{-1}.cm^{-1}$.

Methoxycarbonylation of βLG

Beta-LG (8.5 mg) was dissolved in 20 mM phosphate pH 7.5 (2 mL). DMPC (1 µL) was added to the solution. After 1h at RT, the mixture was submitted to gel filtration as above. Protein concentration was assayed at 280 nm taking ε = 17,600 $M^{-1}.cm^{-1}$.

Synthesis of HEWL•Ir(Cp)*

A solution of HEWL (248 µM in water, 1.5 mL) was mixed with a solution of hydrolysed Ir(Cp*) complex (20 mM in DMSO/H_2O 1/1) to make an Ir/HEWL ratio of 1:1, 5:1 or 10:1. After ca. 2h at RT, the mixture was submitted to gel filtration on a prepacked column (Pierce dextran desalting column, 10 mL, Thermo scientific) using 50 mM HEPES pH 7.8 as eluent. Twelve 1-mL fractions were collected manually and analysed at 280 nm. The fractions containing the protein were pooled were protein concentration was assayed at 280 nm taking ε = 38,000 $M^{-1}.cm^{-1}$.

Catalytic runs with hydrolysed M(arene) and TFACP

This article is protected by copyright. All rights reserved.

Accepted Manuscript

To 1 M HCOONa (1 mL, pH 7.5) were successively added TFACP (5 µmol, 0.7 µL) and the metal complex (0.1 µmol metal out of a 5 mM aqueous solution). Mixtures were incubated at 40°C for up to 33 h and analysed by HPLC to determine the conversion.

Catalytic runs with βLG•M(arene) and TFACP

The solution of βLG•M(arene) (0.1 µmol) was completed to 1 mL with water. Sodium formate (68 mg, 1 M final concentration) and TFACP (5 µmol, 0.7 µL) were successively added. The mixture was incubated at 40°C for up to 33 h and analysed by chiral HPLC over time to determine the conversion and the enantiomeric excess.

Catalytic runs with βLG + Ru(benz) and other aryl ketones

To each ketone (10 µmol) dissolved in DMSO (50 µL) was successively added 1 M HCOONa (1 mL), βLG (0.1 µmol, 2.2 mg) and hydrolysed Ru(benz) (0.3 µmol metal out of a 5 mM solution). The mixture was incubated at 40°C for 40 h. After cooling, the aqueous solution was extracted with isopropyl ether containing 0.1% heptane (v/v) as internal standard (1 mL). The organic phase was analysed by chiral GC to determine the conversion and the enantiomeric excess.

Catalytic runs with HEWL•Ir(Cp) and TFACP*

The solution of HEWL•Ir(Cp*) (0.1 µmol) was completed to 1 mL with 50 mM HEPES pH 7.8. Sodium formate (68 mg, 1 M final concentration) and TFACP (5 µmol, 0.7 µL) were successively added. The mixture was incubated at 40°C for up to 24 h and analysed by chiral HPLC to determine the conversion and the enantiomeric excess at various incubation times.

Catalytic runs with HEWL + hydrolysed M(L) and TFACP

To 1 M HCOONa (1 mL, pH 7.5) were successively added TFACP (10 µmol, 1.4 µL), HEWL (0.2 µmol, 3.2 mg) and hydrolysed M(L) complex (0.2 µmol out of a 5 mM aqueous solution). The mixture was incubated at 40°C for 9 h and analysed by chiral HPLC to determine the conversion and the enantiomeric excess.

Titration of βLG with hydrolysed Ru(benz) monitored by fluorescence spectroscopy

Fluorescence spectra were recorded on a F-6200 spectrofluorometer (JASCO) at 20°C in a 1 cm-path length quartz cuvette between 300 and 430 nm (λ_{ex} = 290 nm) with 5 nm excitation and emission bandwidth, 1 nm data pitch, 125 nm/min scanning rate. An aqueous solution of βLG (5.4 µM) was transferred to the quartz cuvette and small aliquots of hydrolysed Ru(benz) (2 mM in H_2O) were added sequentially to achieve up to 10 equivalents of complex. The blank experiment was performed with a solution of *N*-acetyl-L-tryptophanamide ethyl ester (10 µM) instead of βLG.

Mass spectrometry

ESI-MS experiments were carried out using a LTQ-Orbitrap XL from Thermo Scientific (San Jose, CA, USA) and operated in positive ionization mode, with a spray voltage at 4.5 kV. βLG-A at 5.2 or 10.4 µM under native or reduced forms, respectively, in a

This article is protected by copyright. All rights reserved.

Accepted Manuscript

water/acetonitrile/formic acid 49/50/1 (v:v:v) mixture was continuously infused using a 250 µL syringe at 5 µL/min flow. Applied voltages were 40 and 100 V for the ion transfer capillary and the tube lens, respectively. The ion transfer capillary was held at 275°C. Sheath and auxiliary gas were set at a flow rate of 45 and 15 arbitrary units (a.u.), respectively. Applied voltages were 20 and 70 V for the ion transfer capillary and the tube lens, respectively. The ion transfer capillary was held at 275°C. Detection was achieved in the Orbitrap with a resolution set to 100,000 (at m/z 400) and a m/z range between 200-2000 in profile mode. Spectra were analysed using the acquisition software XCalibur 2.1 (Thermo Fisher Scientific, Courtaboeuf, France) without smoothing and background subtraction. The automatic gain control (AGC) allowed accumulation of up to 2.10^5 ions for FTMS scans, Maximum injection time was set to 300 ms and 3 µscan were acquired. During MS/MS scans, the precursor selection window was set to 2.8 Da and collision-induced dissociation (CID) of 20% was applied with an activation Q value of 0.25 and an activation time of 30 ms. Fragmentation occurred in the linear ion trap analyser (LTQ) and detection in the Orbitrap in profile mode. The automatic gain control (AGC) allowed accumulation of up to 2.10^5 ions for FTMS scans, 1.10^5 ions for FTMSn scans and 1.10^4 ions for ITMSn scans. Maximum injection time was set to 300 ms and 1000 ms for FTMS and FTMSn scans, respectively. For all scan modes, 3 µscan was acquired.

ACKNOWLEDGEMENTS

The Agence Nationale de la Recherche (ANR) is gratefully acknowledged for financial support (project "Artzymes", grant number ANR-11-BS07-027-01). E. Aubry is acknowledged for carrying out the ICP-OES measurements at the METIS laboratory of the UPMC.

Supporting information: Details of chromatographic procedures, NMR and mass spectra and fluorescence titration studies can be found in the supporting information.

References

[1] a) T. Heinisch, M. Pellizzoni, M. Durrenberger, C. E. Tinberg, V. Kohler, J. Klehr, D. Haussinger, D. Baker, T. R. Wardt, *Journal of the American Chemical Society* **2015**, *137*, 10414-10419; b) O. Pamies, M. Dieguez, J. E. Backvall, *Advanced Synthesis & Catalysis* **2015**, *357*, 1567-1586; c) J. Bos, G. Roelfes, *Curr. Op. Chem. Biol.* **2014**, *19*, 135-143; d) J. C. Lewis, *ACS Catal.* **2013**, *3*, 2954-2975; e) A. Onoda, T. Hayashi, M. Salmain, in *BIoorganometallic chemistry* (Eds.: G. Jaouen, M. Salmain), Wiley-VCH, Weinheim (D), **2015**, pp. 305-337.

[2] F. Schwizer, Y. Okamoto, T. Heinisch, Y. Gu, M. M. Pellizzoni, V. Lebrun, R. Reuter, V. Kohler, J. C. Lewis, T. R. Ward, *Chem. Rev.* **2017**.

[3] Y. Lu, N. Yeung, N. Sieracki, N. M. Marshall, *Nature* **2009**, *460*, 855-862.

[4] a) J. Bos, F. Fusetti, A. J. M. Driessen, G. Roelfes, *Angew. Chem. Int. Ed.* **2012**, *51*, 7472-7475; b) D. Coquiere, J. Bos, J. Beld, G. Roelfes, *Angew. Chem. Int. Ed.* **2009**, *48*, 5159-5162; c) P. J. Deuss, G. Popa, A. M. Z. Slawin, W. Laan, P. C. J. Kamer, *ChemCatChem* **2013**, *5*, 1184 – 1191; d) W. Ghattas, L. Cotchico-Alonso, J. D.

This article is protected by copyright. All rights reserved.

Accepted Manuscript

Marechal, A. Urvoas, M. Rousseau, J. P. Mahy, R. Ricoux, *Chembiochem* **2016**, *17*, 433-440; e) T. Himiyama, D. F. Sauer, A. Onoda, T. P. Spaniol, J. Okuda, T. Hayashi, *J. Inorg. Biochem.* **2016**, *158*, 55-61; f) J. Podtetenieff, A. Taglieber, E. Bill, E. J. Reijerse, M. T. Reetz, *Angew. Chem. Int. Ed.* **2010**, *49*, 5151-5155.

[5] a) T. K. Hyster, L. Knorr, T. R. Ward, T. Rovis, *Science* **2012**, *338*, 500-503; b) P. Dydio, H. M. Key, A. Nazarenko, J. Y. E. Rha, V. Seyedkazemi, D. S. Clark, J. F. Hartwig, *Science* **2016**, *354*, 102-106.

[6] a) P. Srivastava, H. Yang, K. Ellis-Guardiola, J. C. Lewis, *Nature Comm.* **2015**, *6*; b) H. M. Key, P. Dydio, Z. Liu, J. Y. E. Rha, A. Nazarenko, V. Seyedkazemi, D. S. Cark, J. F. Hartwig, *ACS Central Sci.* **2017**, *3*, 302-308; c) M. Bordeaux, V. Tyagi, R. Fasan, *Angew. Chem.-Int. Edit.* **2015**, *54*, 1744-1748.

[7] Y.-W. Lin, *Coord. Chem. Rev.* **2017**, *336*, 1-27.

[8] K. Yamamura, E. T. Kaiser, *J. Chem. Soc., Chem. Commun.* **1976**, 830-831.

[9] a) Q. Jing, R. J. Kazlauskas, *ChemCatChem* **2010**, *2*, 953-957; b) Q. Jing, K. Okrasa, R. J. Kazlauskas, *Chem. Eur. J.* **2009**, *15*, 1370-1376; c) K. Okrasa, R. J. Kazlauskas, *Chem. Eur. J.* **2006**, *12*, 1587-1596; d) H. M. Key, D. S. Clark, J. F. Hartwig, *J. Am. Chem. Soc.* **2015**, *137*, 8261-8268.

[10] A. Pordea, *Curr. Opin. Chem. Biol.* **2015**, *25*, 124-132.

[11] N. Fujieda, J. Schatti, E. Stuttfeld, K. Ohkubo, T. Maier, S. Fukuzumi, T. R. Ward, *Chem. Sci.* **2015**, *6*, 4060-4065.

[12] a) J. C. Lewis, *Current Opinion in Chemical Biology* **2015**, *25*, 27-35; b) I. Drienovska, A. Rioz-Martinez, A. Draksharapu, G. Roelfes, *Chem. Sci.* **2015**, *6*, 770-776; c) H. S. Lee, P. G. Schultz, *J. Am. Chem. Soc.* **2008**, *130*, 13194-13195.

[13] a) T. Kokubo, T. Sugimoto, T. Uchida, S. Tanimoto, M. Okano, *J. Chem. Soc. Chem. Commun.* **1983**, 769-770; b) C. Bertucci, C. Botteghi, D. Giunta, M. Marchetti, S. Paganelli, *Adv. Synth. Catal.* **2002**, *344*, 556-562; c) A. Mahammed, Z. Gross, *J. Am. Chem. Soc.* **2005**, *127*, 2883-2887; d) P. Rousselot-Pailley, C. Bochot, C. Marchi-Delapierre, A. Jorge-Robin, L. Martin, J. C. Fontecilla-Camps, C. Cavazza, S. Menage, *ChemBioChem* **2009**, *10*, 545-552.

[14] a) S. Abe, J. Niemeyer, M. Abe, Y. Takezawa, T. Ueno, T. Hikage, G. Erker, Y. Watanabe, *J. Am. Chem. Soc.* **2008**, *130*, 10512-10514; b) Y. Takezawa, P. Bockmann, N. Sugi, Z. Wang, S. Abe, T. Murakami, T. Hikage, G. Erker, Y. Watanabe, S. Kitagawa, T. Ueno, *Dalton Trans.* **2011**, *40*, 2190–2195; c) S. Abe, K. Hirata, T. Ueno, K. Morino, N. Shimizu, M. Yamamoto, M. Takata, E. Yashima, Y. Watanabe, *J. Am. Chem. Soc.* **2009**, *131*, 6958-6960.

[15] H. Tabe, S. Abe, T. Hikage, S. Kitagawa, T. Ueno, *Chem.-Asian J.* **2014**, *9*, 1373-1378.

[16] a) V. Kohler, J. Mao, T. Heinisch, A. Pordea, A. Sardo, Y. M. Wilson, L. Knorr, M. Creus, J.-C. Prost, T. Schirmer, T. R. Ward, *Angew. Chem. Int. Ed.* **2011**, *50*, 10863-10866; b) A. Pordea, M. Creus, J. Panek, C. Duboc, D. Mathis, M. Novic, T. R. Ward, *J. Am. Chem. Soc.* **2008**, *130*, 8085-8088.

[17] X. Wu, C. Wang, J. Xiao, *Platinum Metals Rev.* **2010**, *54*, 3-19.

[18] a) A. Bogevig, I. M. Pastor, H. Adolfsson, *Chem. Eur. J.* **2004**, *10*, 294-302; b) I. M. Pastor, P. Vastila, H. Adolfsson, *Chem. Eur. J.* **2003**, *9*, 4031-4045; c) J. Wettergren, E. Buitrago, P. Ryberg, H. Adolfsson, *Chem. Eur. J.* **2009**, *15*, 5709-5718; d) J. Wettergren, A. B. Zaitsev, H. Adolfsson, *Adv. Synth. Catal.* **2007**, *349*, 2556-2562.

[19] C. Mayer, D. Hilvert, *Eur. J. Org. Chem.* **2013**, 3427-3431.

Accepted Manuscript

This article is protected by copyright. All rights reserved.

[20] a) M. Durrenberger, T. Heinisch, Y. M. Wilson, T. Rossel, E. Nogueira, L. Knorr, A. Mutschler, K. Kersten, M. J. Zimbron, J. Pierron, T. Schirmer, T. R. Ward, *Angew. Chem. Int. Ed.* **2011**, *50*, 3026-3029; b) A. Pordea, M. Creus, C. Letondor, A. Ivanova, T. R. Ward, *Inorg. Chim. Acta* **2010**, *363*, 601-604; c) M. Creus, A. Pordea, T. Rossel, A. Sardo, C. Letondor, A. Ivanova, I. Le Trong, R. E. Stenkamp, T. R. Ward, *Angew. Chem. Int. Ed.* **2008**, *47*, 1400-1404; d) C. Letondor, N. Humbert, T. R. Ward, *Proc. Natl. Acad. Sci. USA* **2005**, *102*, 4683-4887; e) C. Letondor, A. Pordea, N. Humbert, A. Ivanovna, S. Mazurek, M. Novic, T. R. Ward, *J. Am. Chem. Soc.* **2006**, *128*, 8320-8328.

[21] F. W. Monnard, E. S. Nogueira, T. Heinisch, T. Schirmer, T. R. Ward, *Chem. Sci.* **2013**, *4*, 3269-3274.

[22] a) N. Madern, N. Queyriaux, A. Chevalley, M. Ghasemi, O. Nicolotti, I. Ciofini, G. F. Mangiatordi, M. Salmain, *J.. Mol. Cat. B* **2015**, *122*, 314-322; b) N. Madern, B. Talbi, M. Salmain, *Appl. Organomet. Chem.* **2013**, *27*, 6-12.

[23] a) M. V. Cherrier, S. Engilberge, P. Amara, A. Chevalley, M. Salmain, J. C. Fontecilla-Camps, *Eur. J. Inorg. Chem.* **2013**, 3596-3600; b) A. Chevalley, M. V. Cherrier, J. C. Fontecilla-Camps, M. Ghasemi, M. Salmain, *Dalton Trans.* **2014**, *43*, 5482 - 5489; c) A. Chevalley, M. Salmain, *Chem. Commun.* **2012**, *48*, 11984-11986.

[24] G. Suss-Fink, *J. Organomet. Chem.* **2013**, *751*, 2-19.

[25] S. K. Chowdhury, V. Katta, R. C. Beavis, B. T. Chait, *J. Am. Soc. Mass Spectrom.* **1990**, *1*, 382-388.

[26] a) J. Leonil, D. Molle, J. Fauquant, J. L. Maubois, R. J. Pearce, S. Bouhallab, *J. Dairy Sci.* **1997**, *80*, 2270-2281; b) J. Metltretter, J. Wurst, M. Pischetrieder, *J. Agric. Food Chem.* **2013**, *61*, 6971-6981.

[27] S. Ogo, N. Makihara, Y. Watanabe, *Organometallics* **1999**, *18*, 5470-5474.

[28] a) K. Everaere, A. Mortreux, M. Bulliard, J. Brussee, A. V. d. Gen, G. Nowogrocki, J. F. Carpentier, *Eur. J. Org. Chem.* **2001**, 275–291; b) K. J. Haack, S. Hashiguchi, A. Fujii, T. Ikariya, R. Noyori, *Angew. Chem., Int. Ed. Engl.* **1997**, *36*, 285–288; c) F. K. Cheung, A. J. Clarke, G. J. Clarkson, D. J. Fox, M. A. Graham, C. Lin, A. Lorente Crivillé, M. Wills, *Dalton Trans.* **2010**, *39*, 1395–1402; d) N. Pannetier, J. B. Sortais, P. S. Dieng, L. Barloy, C. Sirlin, M. Pfeffer, *Organometallics* **2008**, *27*, 5852–5859; e) S. Y. Liu, L. Y. Xu, C. Y. Liu, Z. G. Ren, D. J. Young, J. P. Lang, *Tetrahedron* **2017**, *73*, 2374–2381.

[29] a) I. W. McNae, K. Fishburne, A. Habtemariam, T. M. Hunter, M. Melchart, F. Wang, M. D. Walkinshaw, P. J. Sadler, *Chem. Commun.* **2004**, 1786-1787; b) M. P. Sullivan, M. Groessl, S. M. Meier, R. L. Kingston, D. C. Goldstone, C. G. Hartinger, *Chem. Commun.* **2017**, *53*, 4246-4249.

[30] A. Casini, G. Mastrobuoni, W. H. Ang, C. Gabbiani, G. Pieraccini, G. Moneti, P. J. Dyson, L. Messori, *ChemMedChem* **2007**, *2*, 631-635.

[31] W. Hu, Q. Luo, X. Ma, K. Wu, J. Liu, Y. Chen, S. Xiong, J. Wang, P. J. Sadler, F. Wang, *Chem. Eur. J.* **2009**, *15*, 6586-6594.

[32] Y. Lin, Y. Huang, W. Zheng, F. Wang, A. Habtemariam, Q. Luo, X. Li, K. Wu, P. J. Sadler, S. Xiong, *J. Inorg. Biochem.* **2013**, *128*, 77-84.

[33] G. Kontopidis, C. Holt, L. Sawyer, *J. Dairy Sci.* **2004**, *87*, 785-796.

[34] E. Wilson Miles, *Methods Enzymol.* **1977**, *47*, 431-442.

[35] D. Mercadante, L. D. Melton, G. E. Norris, T. S. Loo, M. A. Williams, R. C. Dobson, G. B. Jameson, *Biophys. J.* **2012**, *103*, 303-312.

[36] B. Y. Qin, L. K. Creamer, E. N. Baker, G. B. Jameson, *FEBS Lett.* **1998**, *438*, 272-278.

[37] K. C. Cheng, T. Nowak, *J. Biol. Chem.* **1989**, *264*, 19666-19676.

Accepted Manuscript

This article is protected by copyright. All rights reserved.

[38] E. Moreno-Gordaliza, B. Cañas, M. A. Palacios, M. M. Gómez-Gómez, *Anal. Chem.* **2009**, *81*, 3507-3516.
[39] J. Will, A. Kyas, W. S. Sheldrick, D. Wolters, *J. Biol. Inorg. Chem.* **2007**, *12*, 883-894.
[40] E. Michelucci, G. Pieraccini, G. Moneti, C. Gabbiani, A. Pratesi, L. Messori, *Talanta* **2017**, *167*, 30-38.
[41] J. Erales, B. Gontero, J. Whitelegge, F. Halgand, *Biochem. J.* **2009**, *419*, 75-86.
[42] Y. Qi, Z. Liu, H. Li, P. J. Sadler, P. B. O'Connor, *Rapid Commun. Mass Spectrom.* **2013**, *27*, 2028-2032.
[43] H. Li, T.-Y. Lin, S. L. Van Orden, Y. Zhao, M. P. Barrow, A. M. Pizarro, Y. Qi, P. J. Sadler, P. B. O'Connor, *Anal. Chem.* **2011**, *83*, 9507-9515.
[44] R. H. Wills, A. Habtemariam, A. F. Lopez-Clavijo, M. P. Barrow, P. J. Sadler, P. B. O'Connor, *J. Am. Soc. Mass Spectrom.* **2014**, *25*, 662-672.
[45] C. M. Sze, Z. Shi, G. N. Khairallah, L. Feketeova, R. A. J. O'Hair, Z. Xiao, P. S. Donnelly, A. G. Wedd, *Metallomics* **2013**, *5*, 946-954.
[46] H. L. Li, J. R. Snelling, M. P. Barrow, J. H. Scrivens, P. J. Sadler, P. B. O'Connor, *J. Am. Soc. Mass Spectrom.* **2014**, *25*, 1217-1227.
[47] a) S. M. Meier, Y. O. Tsybin, P. J. Dyson, B. K. Keppler, C. G. Hartinger, *Anal. Bioanal. Chem.* **2012**, *402*, 2655-2662; b) R. F. S. Lee, L. Menin, L. Patiny, D. Ortiz, P. J. Dyson, *Anal. Chem.* **2017**.
[48] D. Das, A. Dutta, P. Mondal, *RSC Adv.* **2014**, *4*, 60548-60556.

Accepted Manuscript

This article is protected by copyright. All rights reserved.